Supplemental Materials

Molecular Biology of the Cell

Adhikari *et al*.

Quantitative live-cell PALM reveals nanoscopic Faa4 redistributions and dynamics on lipid droplets during metabolic transitions of yeast

Santosh Adhikari, Joe Moscatelli and Elias M. Puchner*
School of Physics and Astronomy, University of Minnesota, Twin Cities
Physics and Nanotechnology (PAN), 115 Union Street SE, Minneapolis, MN 55455, USA

Supplementary Material

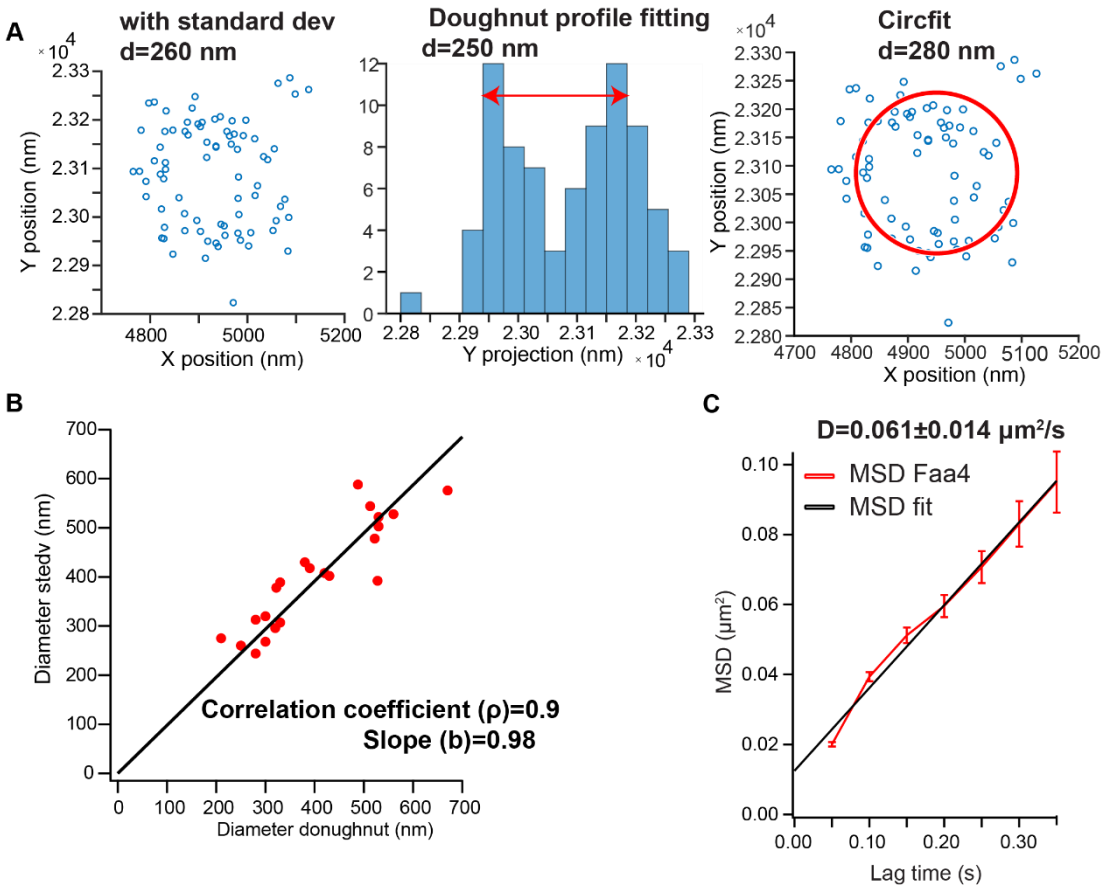

Supplementary Fig 1: LD size quantification and Faa4 single-molecule tracking. (A) Size estimation of a LD using Faa4-mEos2 localizations using averaged standard deviation in x and y (left), donut profile fitting of y projection (middle) and circular fitting (right). (B) Correlation of LD sizes using donut fitting and standard deviation reveals correlation coefficient ρ =0.90 and slope b=0.98. (C) Fitting the average MSD plot of Faa4 traces on the ER and on LDs with a linear function results in a diffusion coefficient of D=0.061± 0.014 μm^2/s. The averaged MSD is calculated from Faa4 traces in 5 cells each containing more than 100 traces lasting at least 3 acquisition frames recorded at 20 Hz. The error of the diffusion coefficient is calculated using the standard deviation of diffusion coefficients from 8 cells.

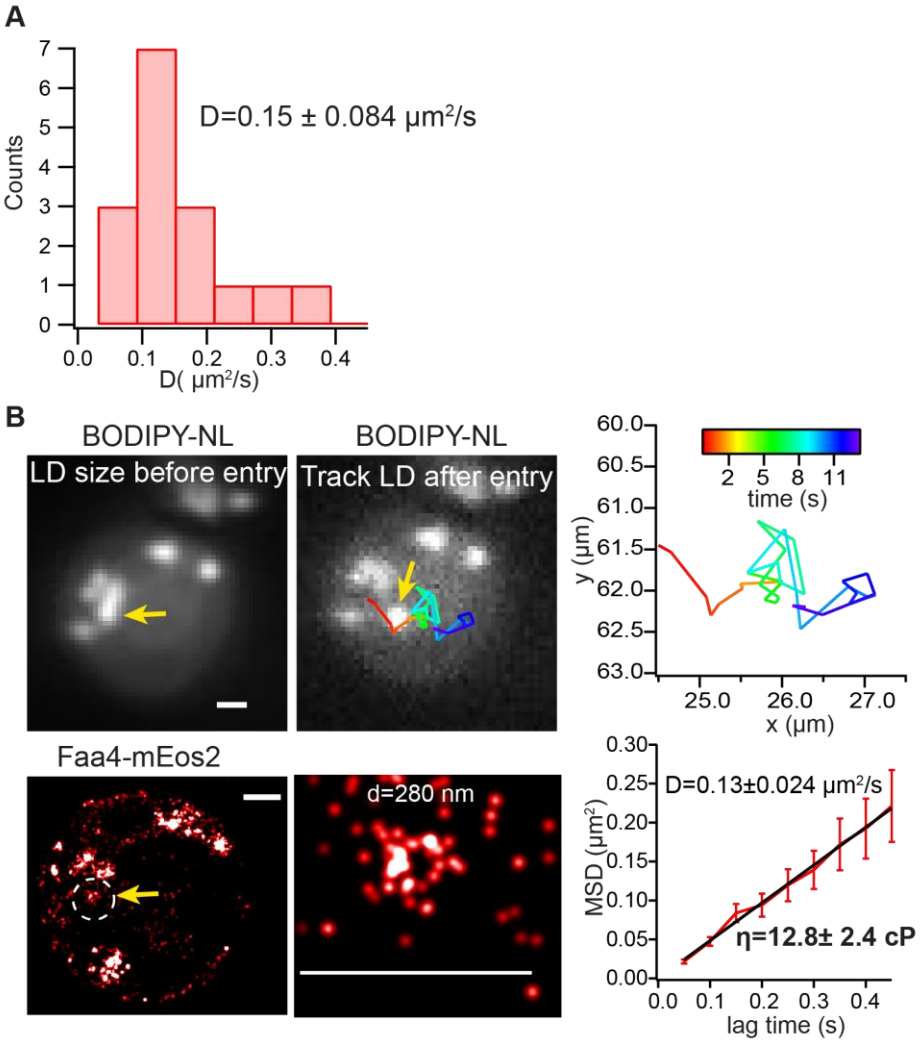

Supplementary Fig 2: Single particle tracking measures LD diffusion inside the vacuole in the stationary phase. (A) Histogram of LD diffusion coefficients calculated from N=16 LDs and 5 cells with a mean of 0.15 ± 0.084 μm^2/s. The error of the diffusion coefficient is calculated using the standard deviation of diffusion coefficients from all LDs. (B) Conventional fluorescence image of BODIPY-NL (top, left) shows LDs in cluster. (Bottom, left) PALM image of LDs clustered around the vacuole. Zoom shows a super-resolved LD with a diameter of d=280 nm before entry into the vacuole. (Top, right) After the LD marked by an arrow enters the vacuole, it randomly diffuses in the vacuolar lumen with a diffusion coefficient of D=0.13 ± 0.024 μm^2/s (bottom, right). The vacuolar viscosity of 12.8 ± 2.4 cP was calculated with an LD size of d=280 nm and diffusion coefficient of D= 0.13 ± 0.024 μm^2/s using the Stokes-Einstein equation. Scale bar: 1 μm

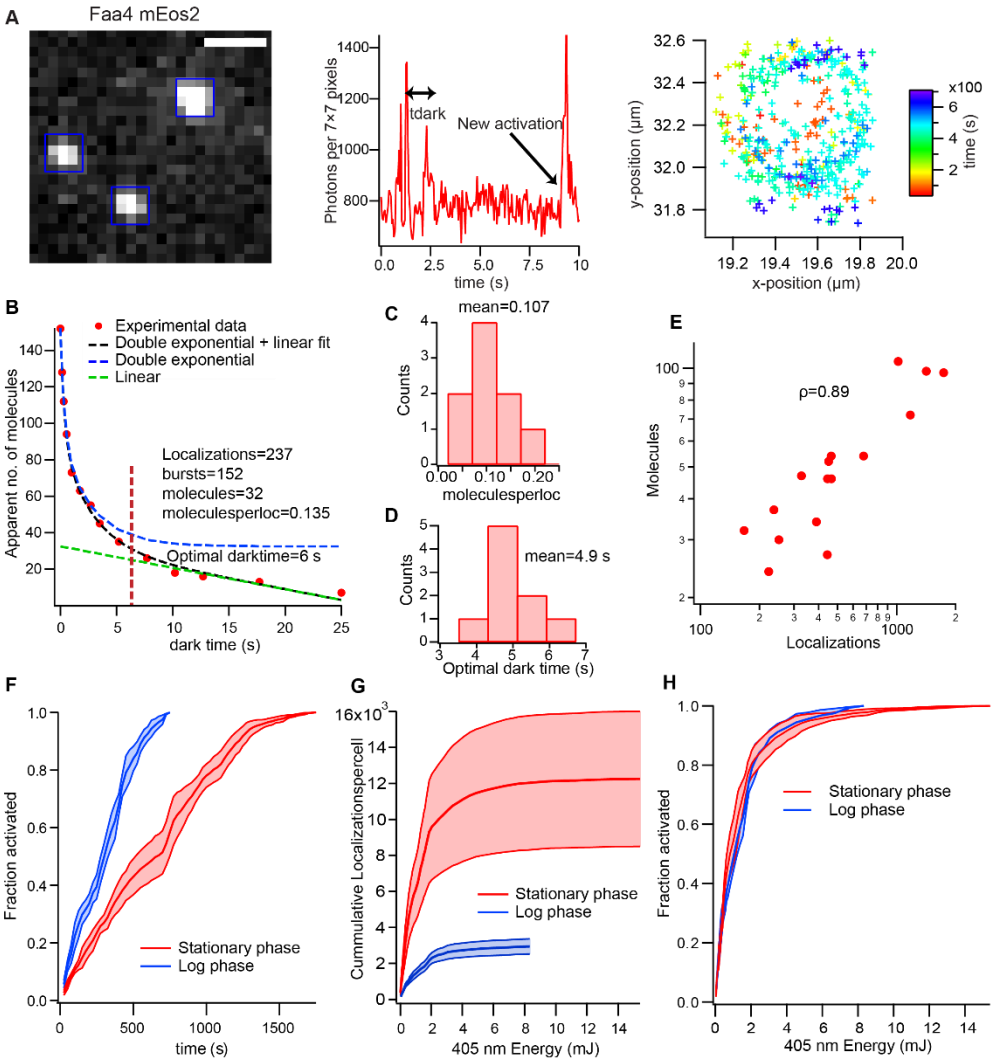

Supplementary Fig 3: Quantification of Faa4-mEos2 molecule numbers on LDs in living cells. (A) A typical raw data acquisition frame (left) with sparse mEos2 localizations. Intensity trace (middle) of a 7×7 pixels region showing blinking of a mEos2 molecule and a newly excited molecule. mEos2 localizations (right) color-coded by frame number on a LD reveal temporally close fluorescent bursts from single mEos2 molecules dispersed on the surface. The diffusion of single mEos2 molecule during the dark time due to blinking leads to dispersed localizations on the LD surface. (B) Number of apparent blink corrected mEos2 molecules (red dots) as a function of allowed dark time t_d for a LD. The number of apparent molecule is obtained by grouping localizations on the LD that appear within the specified dark times and within the maximum diameter of LDs of 650 nm. Apparent molecules at t_d=0s represent the number of fluorescent bursts. Apparent molecules vs dark time show a double exponential decay (dominant at shorter dark times due to blinking) and linear decrease (dominant at longer dark time due to false grouping). The black dotted curve is the fit of the sum of a double exponential decay and a linear function. The blue curve shows only double exponential decay of molecules that converges to actual number of molecules on the LD. The green curve shows linear

decrease of molecules due to false linking (shifted in y by the number of molecules to show convergence with the data at long lag times). The optimal dark time (6 s) balances the over counting fraction from the double exponential part by the undercounting fraction from linear part. The number of molecules per localization (0.135) is obtained from total localizations and the obtained number of blink corrected molecules from the fit at the optimal dark time. (C) Distribution of optimal dark times from N=9 different LDs with varying number of localizations with the mean optimal dark time of 4.9 s. (D) Distribution of molecules per localizations for N=9 different LDs with the mean of 0.107±0.04. (E) Number of molecules vs localizations for N=16 LDs shows strong correlation (ρ=0.89). The strong correlation validates the approach of finding the number of detected localizations per mEos2 molecule for blink correction using detected localizations. (F) Fraction of total mEos2 localizations vs data acquisition time under two different activation schemes for cells in the log phase (low Faa4-mEos2 expression level) and stationary phase (high Faa4-mEos2 expression level). Due to the lower expression level of Faa4-mEos2, most molecules in log-phase cells can be imaged faster compared to cells in the stationary phase. (G) The number of localizations per cell (5 cells for log and 4 cells for stationary phase) vs 405 nm energy delivered in the log and stationary phase. Error band represents standard error on mean. (H) Fraction of localized molecules vs 405 nm energy shows that fraction of localized molecules only depends on the delivered 405 nm photo-activation energy. Error band represents standard deviation calculated from N=5 cells for both log and stationary phase. Scale bar: 1μm.

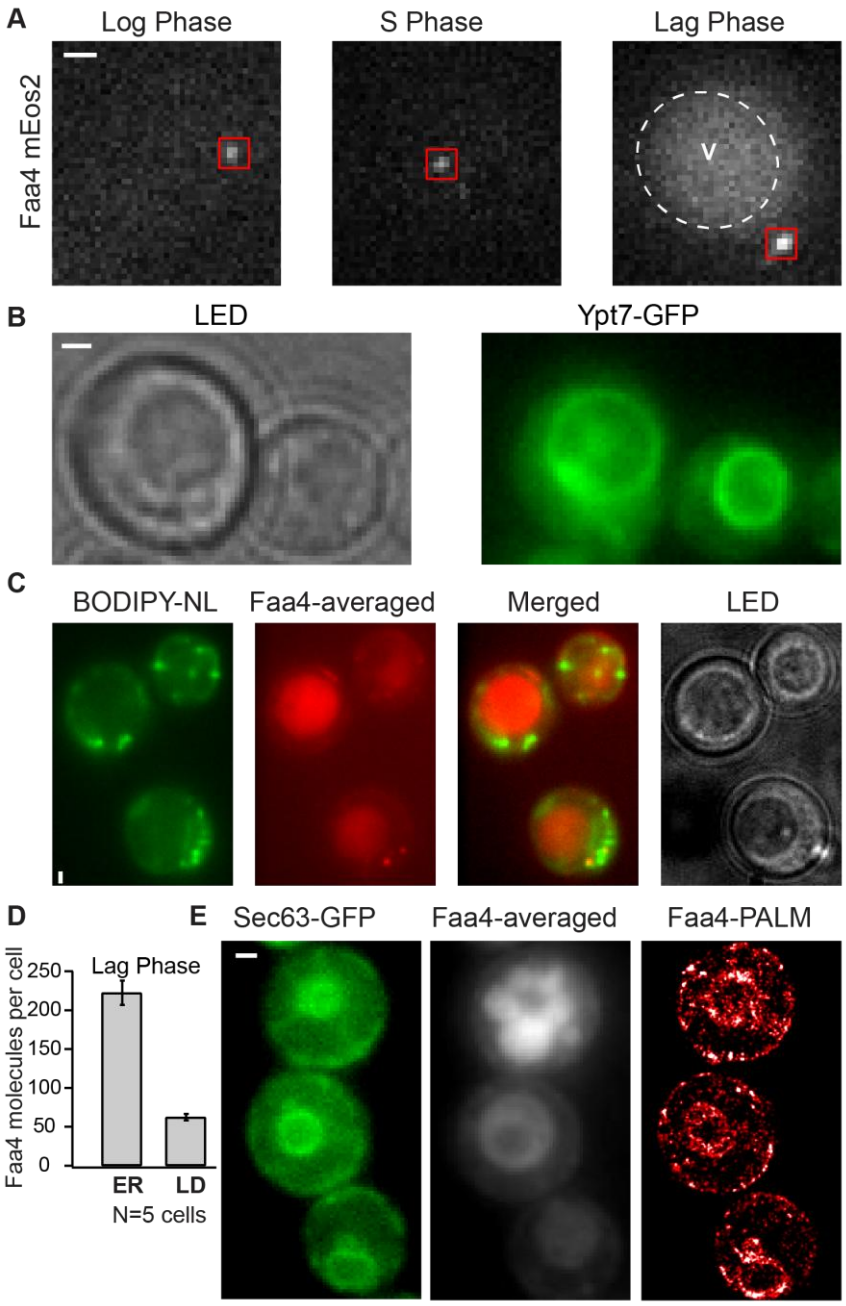

Supplementary Fig 4: Faa4 is predominately localized to the vacuolar lumen in the lag phase. (A) Single frames of Faa4-mEos2 in the log (left), stationary (middle) and lag (right) phase. Fast diffusion of mEos2 in the vacuole creates a diffuse background fluorescence in the lag phase. (B) Transmitted light image (left) and Ypt7-GFP (right) shows that the darker region in the transmitted light image is the vacuole. (C) BODIPY-NL (left), Faa4-mEos2 avg (middle), merged and LED (right) images show LDs not co-localized with the vacuole. Diffused Faa4 signal comes from dark vacuolar region in the LED image. (D) Quantification of the number of Faa4 molecules in ER and on LDs during the lag phase. (E) The conventional fluorescence of Sec63-GFP (left), Faa4-mEos2 averaged (middle) and Faa4-mEos2 PALM (right) after 30 mins

of dilution in fresh medium. A portion of Sec63-GFP signal is seen completely inside Faa4-avg signal from vacuole. Scale Bar: 1 µm

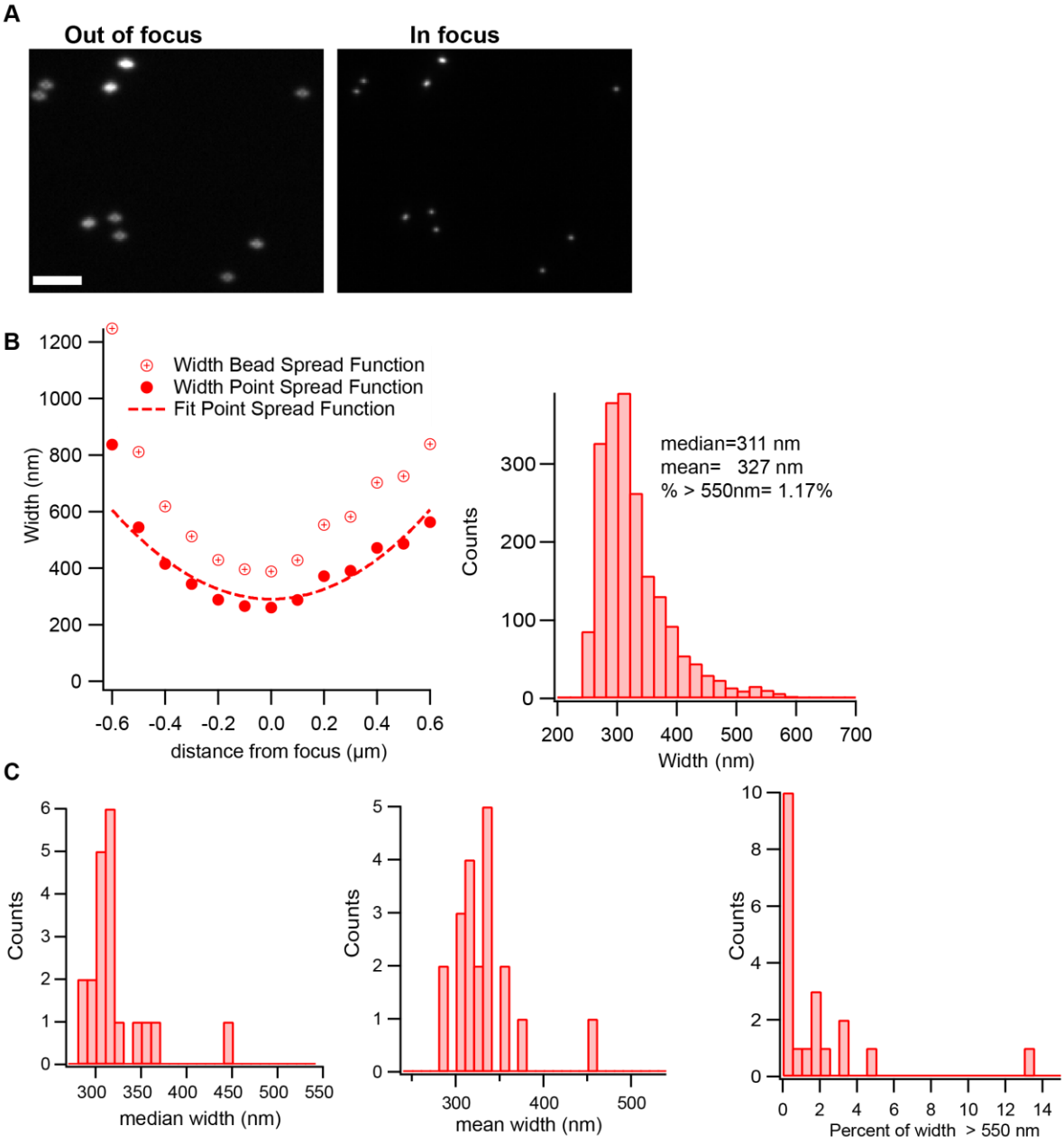

Supplementary Fig 5: Z calibration using PSF width fitting: (A) Fluorescence images of TetraSpeck microsphere beads out of focus (left) and in focus (right) reveal increase in Bead Spread Function (BSF) width for out of focus beads. (B) Width of Bead Spread Function (BSF) of TetraSpeck beads and corresponding PSF shows dependence of the PSF width on the location in z (left). Histogram of localization widths of mEos2 from individual LDs (N=20) show only ~1% of localizations with width greater than 550 nm corresponding to 500 nm away from focus, which is well within our detectable z-range. (C) Histogram of the median (left) and mean (middle) widths of PSF of mEos2 localizations from individual LDs. Right**:** Distribution of percent of mEos2 with PSF widths >550 nm from individual LDs reveals more ~95% of LDs have less than 5% of localizations with width > 550 nm. Scale bar: 1 µm

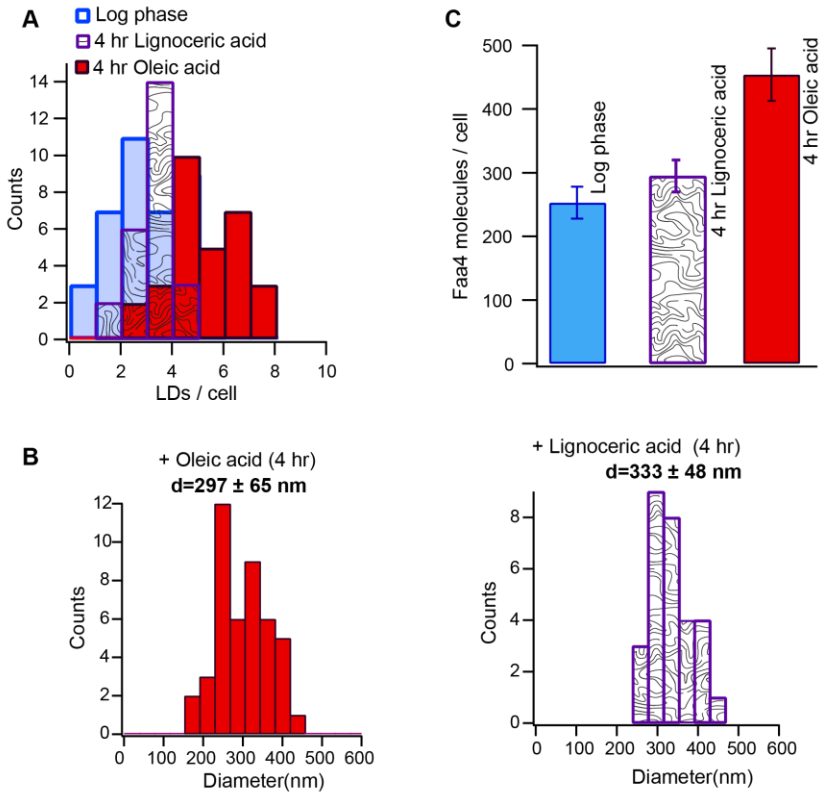

Supplementary Fig 6: **Subcellular localization and density of Faa4 on LDs in the presence of exogenous fatty acids**. (A) Quantification of number of LDs per cell from cells in log phase (N=38 cells) and from cells grown the presence of oleic (N=30 cells) acid lignoceric acid (N=25 cells). (B) Histogram of LD sizes (mean ± s.d) and representative super-resolved LDs from cells grown in the presence of oleic acid (left) and lignoceric acid (right). (C) Quantification of Faa4 molecules per cell from cells in the log phase (N=9 cells) and from cells grown in the presence of oleic acid (N=34 cells) and lignoceric acid (N=17 cells). Error bars represent standard error on mean.